

Structural Features of Nanostructured Copper Oxide Thin Films, Synthesized by Spray Pyrolysis Technique

O.V. Diachenko^{1,*}, A.S. Opanasuyk¹, A.O. Salohub¹, D. Nam², H. Cheong², Yu.P. Gnatenko³

¹ Sumy State University, 2, Rymsky Korsakov Str., 40007 Sumy, Ukraine

² Department of Physics, Sogang University, Seoul 121-742, South Korea

³ Institute of Physics of National Academy of Sciences of Ukraine, Nauky Ave. 46, UA-03028 Kyiv, Ukraine

(Received 01 August 2015; published online 22 August 2015)

In the present study, the properties of copper oxide thin films prepared by spray pyrolysis were investigated at different substrate temperatures (573 – 723 K) and at constant spraying volume of precursor. The compositions, structural and morphological properties of the films were investigated by field emission scanning electron microscopy, atomic force microscopy and Raman spectroscopy.

Keywords: Copper oxide, Raman, atomic force microscope, Thin films, Structure, Spray pyrolysis, Optoelectronic devices, Solar cells.

PACS numbers: 81.05.Dz, 81.15.Rs

1. INTRODUCTION

The rapid development of semiconductor technologies require application an ever various materials with different physical, electrical and optical properties. Therefore, increasing attention is being paid to studies on less known chemical compounds able to act as semiconductors. Among them, compounds of metals with oxygen may be considered as most promising [1].

There are many technics have been used to grown oxide thin films molecular beam epitaxy [2], vapor phase epitaxy [3] electrochemically deposition [4], plasma evaporation method [5], sol-gel synthesis [6], reactive sputtering [7], pulsed laser deposition [8], chemical vapor deposition [9], metal – organic chemical vapor deposition [10], spray pyrolysis [11], etc. Spray pyrolysis has been shown as effective method for obtaining high quality thin films of oxides. This is a very simple and relatively cost-effective processing method (especially with regard to equipment costs) in comparisons to many other film deposited technique which allows to prepare both thin and thick films. It offers an extremely easy technique for preparing films of any composition.

Copper oxide is one of the most promising oxide materials because of its favorable properties in wide range of applications. This compound can be used in diodes [12], field emitters, gas sensors [13], optical switches, magneto resistance materials, catalysts, high temperature superconductors [14] and soil lignin study [15]. The narrow band gap of this material (1.2 eV) favors its use in photoconductive and photothermal applications, optoelectronic devices and solar cells [16-19]. Moreover, this oxide also is an important material for the fabrication of lithium ion battery [20]. For these applications CuO are technologically interesting due to the chemical and physical properties of this material depend on its composition, structure, phase, shape, size, and size distribution [21].

A low production cost and excellent stability at room temperature, non-toxic nature of the copper oxide

material makes it an attractive option for these applications, good hole mobility, large minority carrier diffusion length, and a direct energy gap ideal for efficient absorption.

Synthesizing copper oxides of preferred phase still poses a challenge. The two possible phases of this oxide are copper oxide (CuO) and cuprous oxide (Cu₂O) of monoclinic and cubic structures with band gap values of 1.3 – 2.1 eV and 2.0 – 2.6 eV respectively [22].

2. EXPERIMENTAL DETAILS

Copper oxide thin films were obtained by spray pyrolysis method used laboratory system described in details in [11]. For sample preparation, the 1x1 cm² glass substrates of thickness 1 mm were ultrasonically cleaned with pure water and ethanol for 6 minutes. 0.05 molar of copper chloride (CuCl₂·2H₂O) were dissolved in 100 mL of deionized water under constant stirring. Note, that most authors of previous works have studied copper oxide thin films obtained from solution based on copper acetate [14, 23-27] or copper nitrate [28, 29]. The precursor solution was sprayed using a jet nozzle using air as the carrier gas on to heated substrate. The diameter of the nozzle is 0.2 mm. The distance between the nozzle and the heated substrate surface was equal to 15 cm. Spraying rate was 2 ml/min and the volume of sprayed solution of 3 ml per sample. The substrate temperature range for synthesis of the films was changed from $T_s = 573$ K to 723 K with step $\Delta 50$ K. The substrates temperature during the obtaining of films was measured using a chromel-alumel thermocouple.

Field emission scanning electron microscope JEOL JSM-7600F was used to investigate morphological properties of the obtained layers.

The thickness of the samples was determined using by a probe Profilers Dektak XT. Measurements were carried out relative to the area of the substrate without a copper oxide layer. During the measurements were used next experimental conditions: scan length – 2000

* alexey.dyachenko@ukr.net

μm , resolution – 0.666 μm , stylus force – 3 mg, stylus scan range – 65.5 μm

The surface morphology was probed using atomic force microscopy (AFM). The scanning area was $50 \times 50 \mu\text{m}$. Non-contact mode was used during the measurements. RMS were calculated using AFM data analysis software.

Macro-Raman spectroscopy enables fast, large area Raman mapping needed for statistical studies of materials properties. Raman spectroscopy measurements were carried out in ambient conditions with the 441.6 nm-line of a He-Cd laser as excitation source. A laser beam with a power of ~ 20 mW was focused to a line of $\sim 5 \text{ mm} \times 50 \mu\text{m}$ in a quasi-backscattering configuration. Jobin-Yvon TRIAX 550 spectrometer (2400 grooves/mm) was used to disperse the signals. The measurement range was up to 700 cm^{-1} . The slit width was fixed at 0.1 mm. An long-wave-pass (LWP) edge filter lens was used to eliminate the laser signals. A spike lens was also used. The signals were detected with a liquid-nitrogen-cooled back-illuminated charge-coupled-device detector array.

3. RESULT AND DISCUSSION

Micrographs of obtained thin films are shown on figure 1. As see from the figure the films have polycrystalline structure. With increasing substrate temperature crystal size are generally decreasing from 1 μm ($T_s = 573 \text{ K}$) to 20 nm ($T_s = 673 \text{ K}$). However, at higher synthesis temperatures grain size films grew reaching 1.5-2.0 μm in the layers obtained at $T_s = 723 \text{ K}$. The crystallites of the samples synthesized at low temperatures had cubic shape.

The surface profiles were investigated using by a probe Profilers Dektak XT. There are three measurements of each sample were held. Initially, the average profile graph was found by using OriginPro software packet followed by a shift of the graphs with respect to minimum point to zero in y-axis direction. Minimum point is a glass substrate without film layer. Thus it is possible to measure the thickness of the sample. Established that the average thickness of the samples ranged from 0.8 μm at $T_s = 723 \text{ K}$ to 2.2 μm at $T_s = 573 \text{ K}$.

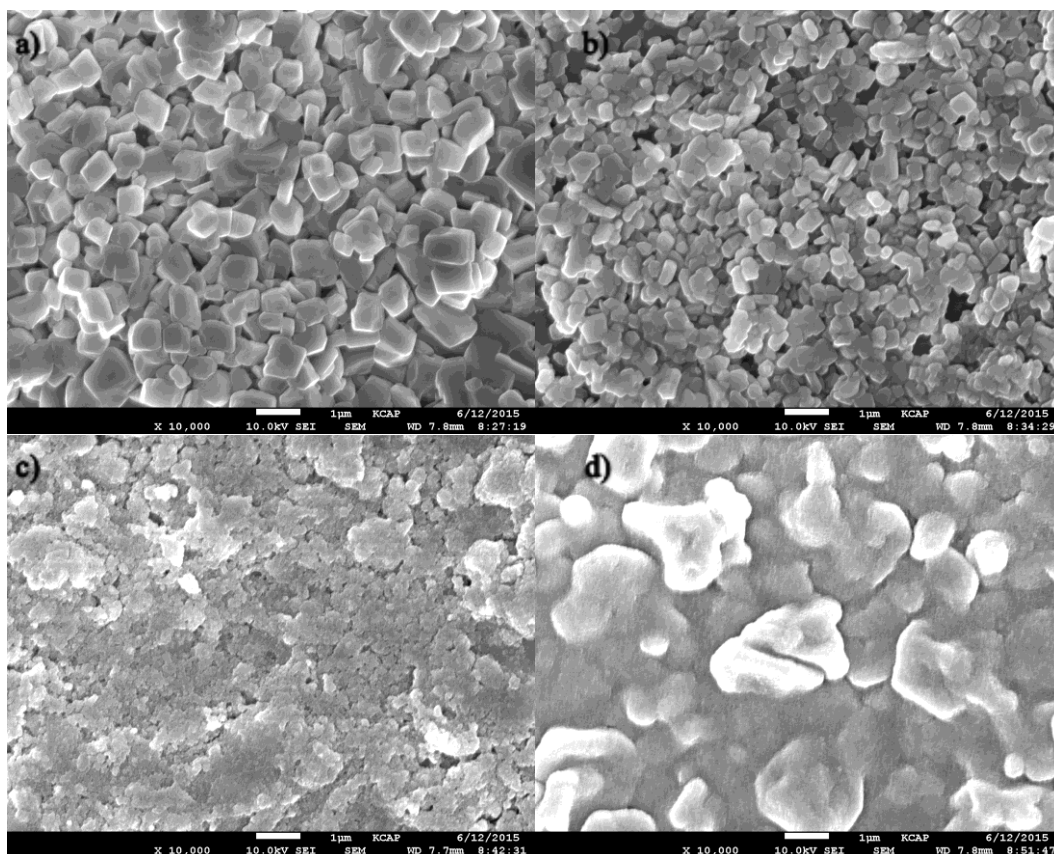


Fig. 1 – FESEM images of samples obtained at $T_s = 573 \text{ K}$ (a), 623 K (b), 673 K (c), 723 K (d).

AFM images of copper oxide thin films are shown in Fig. 2. Obtained films show uniform surface with closely packed microstructure all over the substrate. The similar surface texture has been observed by Yasui et al. [22].

Copper Oxide (CuO) is a compound which crystallizes in a monoclinic crystal structure where Cu^{2+} ions are fourfold coordinated by oxygen and described by the space group C_2^h ($C 2/c$) [30-31]. There are four molecular units in the crystallographic unit cell and only two in the

primitive cell. Since two molecular units in the primitive cell there are 12 vibrational modes at the zone center. The two Cu atoms in the primitive cell are on sites with symmetry described by $C_1(2)$ and the oxygen atoms on C_2 (2) [30].

There are 12 zone-center optical-phonon modes $\Gamma_{\text{RA}} = 4A_u + 5B_u + A_g + 2B_g$, where Γ is the degree of vibrational freedom, A_u and B_u represent Infrared modes; A_g and B_g represents Raman modes. There are six infrared active modes ($3A_u + 3B_u$), three acoustic modes ($A_u +$

2B_u), and three Raman active modes (A_g + 2B_g) [32-34].

Figure 3 shows the Raman spectra of copper oxide films. In comparison with the vibrational spectra of CuO powder [35], single crystals [36], nanoparticles [33, 37] and nanostructures [32, 34] we can assign the peak at 274 cm⁻¹ to the A_g mode and the peak at 327 cm⁻¹ to the B_g modes. The peak at 616 cm⁻¹ that correspond to the B_{2g} mode didn't detect since it has weak natural. Also the peak at 486 cm⁻¹ assigned to the 2E_u mode of Cu₂O. These wavenumbers are close to those reported in the

literature [32-38]. They reported that the intensity is related to the grain size. Stronger and sharper Raman peaks are observed which also shift to longer wavenumbers with increasing or decreasing grain size. Our results are in agreement with the previously reported data. There are several peaks at wavenumbers range from 100 cm⁻¹ to 250 cm⁻¹ can be assigned to the bending vibrations of CuO₂ and CuO₄ clusters [37].

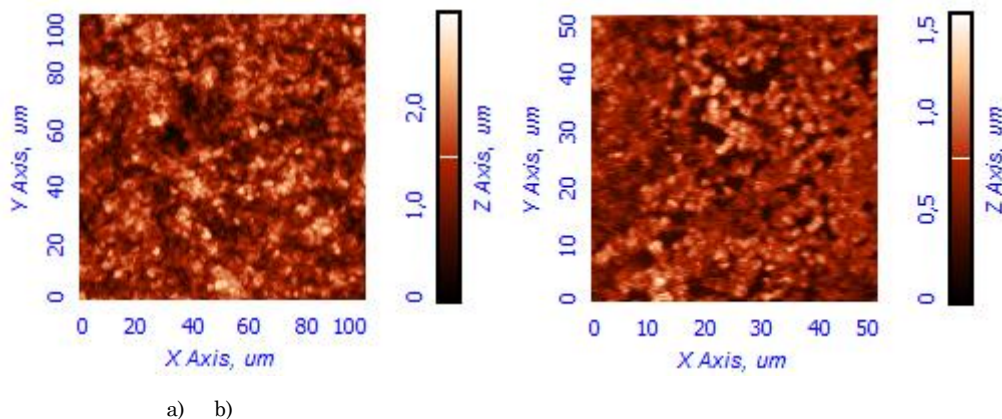


Fig. 2 – AFM images of copper oxide thin films obtained at $T_s = 643$ K (a), 653 K (b)

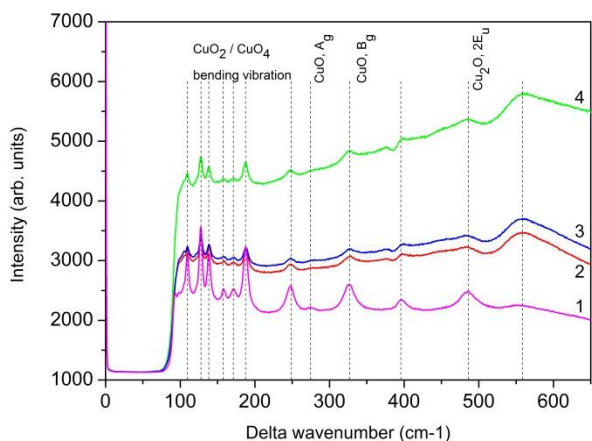


Fig. 3 – Raman spectra of copper oxide thin films obtained at $T_s = 573$ K (1), 623 K (2), 723 K (3), 673 K (4).

4. CONCLUSIONS

Homogeneous and single phase nanostructured MgO films have been obtained by a simple and cost effective spray pyrolysis method. Copper chloride

(CuCl₂·2H₂O) used as a precursor. Optical and morphological properties of MgO thin films have been investigated by field emission scanning electron microscopy, atomic force microscopy and Raman spectroscopy.

It found that the copper oxide thin films have uniform surface with closely packed microstructure with a grain size of 20 nm - 2 μm and have low roughness. The surface roughness was also calculated. It was established that the average thickness of the samples ranged from 0.8 μm at $T_s = 723$ K to 2.2 μm at $T_s = 573$ K. According to Raman spectroscopy the samples have CuO phase with impurities of Cu₂O phase.

Thus, the layers of copper oxide can be used in optoelectronic devices and solar cell as optical window material with p-type conductivity.

ACKNOWLEDGEMENTS

This research was supported by the Ministry of Education and Science of Ukraine (Grant No. 0113U000131 and 0112U000772) and the International Research & Development Program of the National Research Foundation of Korea (NRF) funded by the Ministry of Education, Science and Technology (MEST) of Korea.

REFERENCES

1. Z.M. Jarzebski, *Oxide Semiconductors* (Pergamon Press: Oxford: 1973).
2. M.S. Kim, et al., *J. Korean Phys. Soc.* **59**, 2354 (2011).
3. S.S. Lee, et al., *Proc. of the Fifteenth International Symposium on Chemical Vapor Deposition* **200**, 277 (2000).
4. A. Kathalingam, et al., *J. Korean Phys. Soc.* **55**, 2476 (2009).
5. K. Santra, et al., *Thin Solid Films* **213**, 226 (1992).
6. J.G. Yoon, H.K. Kim., *J. Korean Phys. Soc.* **31**, 613 (1997).
7. Y.S. Yoon, J.S. Kim, S.H. Choi, *Thin Solid Films* **460**, 41 (2004).
8. I. Bouessay, A. Rougier, J.M. Tarascon, *Electrochrom. Mater. Appl.: Proc. Int. Symp.*, 91 (2003).
9. T. Maruyama, S. Arai, *J. Electrochem. Soc.* **143**, 1383 (1996).
10. J.H. Boo, et al., *Thin Solid Films* **341**, 63 (1999).
11. A.V. Dyachenko, et al., *NAP Proc.* **3**, 01PCSI05 (2014).

12. İ.Y. Erdoğan, Ö. Güllü, *J. Alloys Compnds* **492**, 378 (2010).
13. A. Chowdhuri et al., *Appl. Phys. Lett.* **84**, 1180 (2004).
14. V. Saravanan, et al., *J. Anal. Appl. Pyrolysis* **62**, 327 (2014).
15. M.F. Dignac et al., *J. Anal. Appl. Pyrolysis* **85**, 426 (2009).
16. H. Kidowaki, et al., *J. Mater. Sci. Res.* **1**, 138 (2012).
17. V. Kumar, et al., *Nanoelectronics Conference (INEC), 2013 IEEE 5th International*, 443 (2013).
18. S. Gubbala, J. Thangala, M.K. Sunkara, *Sol. Energ. Mat. Sol. Cells* **9**, 813 (2007).
19. H.D. Banerjee, et al., *Opt. Eng.* **27**, 271133 (1988).
20. P. Poizot, et al., *Nature* **407**, 496 (2000).
21. A.P. Moura, et al., *Adv. Powder Tech.* **21**, 197 (2010).
22. T. Maruyama, *Sol. Energ. Mat. Sol. Cells* **56**, 85 (1998).
23. W. DeSisto, et al., *Mater. Res. Bull.* **6**, 753 (1989).
24. J. Morales, et al., *Electrochim, Acta* **29**, 4589 (2004).
25. T. Kosugi, S. Kaneko, *J. Am. Ceram. Soc.* **12**, 3117 (1998).
26. K. Rajaram, E. Savarimuthu, S. Arumugam, *Res. J. Mater. Sci.* **2320**, 6055 (2013).
27. J. Morales, et al., *Thin Solid Films* **474**, 133 (2005).
28. D. Majumdar, et al., *J. Mater. Res.* **11**, 2861 (1996).
29. C.Y. Chiang, et al., *Int. J. Hydr. Energ.* **24**, 15519 (2011).
30. S. Asbrink., L.J. Norrby, *Acta Cryst. B* **26**, 8 (1970).
31. M. Heinemann, B. Eifert, C. Heiliger, *Phys. Rev. B* **11**, 115111 (2013).
32. K. Mageshwari, R. Sathyamoorthy, *J. Mater Sci. Tech.* **29**, 909 (2013).
33. S.K. Maji, et al., *J. Solid State Chem.* **8**, 1900 (2010).
34. X. Wang, et al., *Crystal Growth* **5**, 930 (2007).
35. W. Reichardt, et al., *Zeit. Phys. B* **81**, 19 (1990).
36. J. Chrzanowski, J.C. Irwin, *Solid State Comm.* **70**, 11 (1989).
37. T. Baruah, R.R. Zope, M.R. Pederson, *Phys. Rev. A* **69**, 023201 (2004).
38. M. Rashad, et al., *J. Nanomater.* **13**, 82 (2013).